Genome-wide screen for deficiencies modifying *Cyclin G*-induced developmental instability in *Drosophila melanogaster*

Valérie Ribeiro[1], Marco Da Costa[1], Delphine Dardalhon-Cuménal [1], Camille A. Dupont[1], Jean-Michel Gibert[1], Emmanuèle Mouchel-Vielh[1], Hélène Thomassin[1], Neel B. Randsholt[1], Vincent Debat[3*] and Frédérique Peronnet[1]*

[1] Sorbonne Université, CNRS, Inserm, Développement Adaptation et Vieillissement, Dev2A, F75005 Paris, France

[2] Sorbonne Université, CNRS, Inserm, Institut de Biologie Paris-Seine, IBPS, F75005 Paris, France

[3] Institut de Systématique, Evolution, Biodiversité (ISYEB), Muséum national d'Histoire naturelle, CNRS, Sorbonne Université, EPHE, Université des Antilles CP 50, 57 rue Cuvier, 75005 Paris, France

*** Correspondence:**

Co-last and co-corresponding Author

frederique.peronnet@sorbonne-universite.fr

vincent.debat@mnhn.fr

Running title: Developmental stability

Keywords: Developmental instability, Drosophila, Fluctuating asymmetry (FA), Cyclin G, Genetic screen

ABSTRACT

Despite long-lasting interest and research efforts, the genetic bases of developmental stability – the robustness to developmental noise – and its most commonly used estimator, fluctuating asymmetry (FA), remain poorly understood. The *Drosophila melanogaster Cyclin G* gene (*CycG*) encodes a transcriptional cyclin that regulates growth and the cell cycle. Over-expression of a potentially more stable isoform of the protein (deleted of a PEST-rich domain, hereafter called $CycG^{\Delta P}$) induces extreme wing size and shape FA (*i.e.* high developmental noise), indicating a major disruption of developmental stability. Previous attempts to identify the genetic bases of FA have been impeded by the constitutively low level of developmental noise, strongly limiting the power to detect any effect. Here, we leverage the extreme developmental instability induced by overexpression of $CycG^{\Delta P}$ to explore the genetic bases of FA: we perform a genome-wide screen for deficiencies that enhance or reduce $CycG^{\Delta P}$-induced wing FA. 499 deficiencies uncovering 90% of the euchromatic genome were combined with a recombinant chromosome expressing $CycG^{\Delta P}$. We identified 13 and 16 deficiencies that enhance and decrease FA, respectively. Analysis of mutants for some genes located in these deficiencies shows that Cyclin G ensures homogeneous growth of organs in synergy with the major morphogens of the wing, Dpp and Wg, as well as the Hippo and InR/TOR pathways. They also reveal that $CycG^{\Delta P}$-induced FA involves Larp, a potential direct interactor of Cyclin G, that regulates translation at the mitochondrial membrane. This opens up new research perspectives for understanding developmental stability, suggesting a significant role for mitochondrial activity.

INTRODUCTION

Developmental noise results from the inherent variability of biological processes, that operates independently of genetic or environmental factors (for a review on concepts see (Debat 2001)). Developmental stability refers to the buffering of developmental noise. In bilaterians, an estimate of developmental noise is provided by fluctuating asymmetry (FA), which refers to slight, random deviations from perfect symmetry in paired structures, such as bilateral organs. The genetic bases of developmental stability remain largely unknown. Investigation of mandible size and shape FA in a population of mice has identified a few single-locus Quantitative Loci Traits (QTLs) (Leamy et al. 2015). In *Drosophila*, the wings, which have a highly stereotyped organisation, are commonly used to measure FA, the variance in the difference between the left and right wing in a population. Genome-wide deficiency mapping of regions responsible for developmental noise has identified deficiencies associated with increased centroid size or shape FA (Takahashi, Okada, Teramura, et al. 2011; Takahashi, Okada, and Teramura 2011). However, the consistently low level of developmental noise - which greatly limits the ability to detect any effects - likely explains why no attempts have been made to identify the genes responsible for these effects within the QTLs or deficiencies.

In *Drosophila melanogaster,* the *Cyclin G* gene (*CycG*), which encodes a transcriptional cyclin, has been implicated in developmental noise (Debat et al. 2011; Debat and Peronnet 2013). Indeed, overexpression of $CycG^{\Delta P}$, a modified version of Cyclin G that lacks the C-terminal PEST domain and is therefore potentially more stable, induces an unprecedented high level of size and shape FA (40-fold increase compared to control). The strongly destabilized system induced by $CycG^{\Delta P}$ overexpression offers a unique opportunity to investigate the genetic bases of developmental stability. In this study we used $CycG^{\Delta P}$ overexpression to perform a genome-wide screen for deficiencies that enhance or reduce $CycG^{\Delta P}$-induced wing size FA. 495 deficiencies uncovering about 90% of the euchromatic genome were combined with a recombinant chromosome expressing $CycG^{\Delta P}$. We thus identified 13 deficiencies that enhance FA and 16 deficiencies that decrease it. Analysis of mutants for some genes located in these deficiencies shows that Cyclin G ensures homogeneous growth of organs in synergy with morphogens and growth control pathways. They also suggest an impact of mitochondrial activity on developmental stability.

MATERIAL AND METHODS

Genetics

Flies were raised in yeast-cornflour broth (yeast extract 75 g/L, cornflour 90 g/L, agar-agar 10.7 g/L, methyl 4-hydroxybenzoate 5.5 g/L) at 25°C. Lines carrying deficiencies (*Df*) were obtained from the Bloomington stock center (Supplementary Table 1). These lines have been generated in two different w^{1118} genetic backgrounds (stocks BL-5905 and BL-6326) that were used as negative controls (further called w^{5905} and w^{6326}, respectively). The mutant alleles used in this study are listed in Supplementary Table 2. The *da-Gal4,UAS-CycG*$^{\Delta P}$ third chromosome, obtained by genetic recombination (Debat et al. 2011), was used as a positive control. Due to high lethality and low fertility, this chromosome was maintained against the *TM6c,Sb* balancer, in males, at 18°C.

In order to address the genetic interactions between *CycG* and each deficiency, 5 replicate crosses containing 6 deficiency or control females and 5 *da-Gal4*, *UAS-CycG*$^{\Delta P}$*/TM6c, Sb* or *da-Gal4* males were performed. Series of experiments with up to 25 deficiencies were performed, each series including the appropriate positive and negative controls. Care was taken to keep the crosses in standardized conditions: tubes used for a given series were from the same batch, they were maintained at 25°C on the same incubator floor, parents were transferred into new tubes each 48 h, three times, then discarded. The offspring was counted and kept in 70 % ethanol. Thirty females of the desired genotype (*Df/da-Gal4*, *UAS-CycG*$^{\Delta P}$, *+/da-Gal4*, *UAS-CycG*$^{\Delta P}$, *Df/da-Gal4* or *+/da-Gal4*) were randomly sampled (Supplementary Figure 1).

Measurements and statistical analysis

The wings were mounted and scanned as described (Debat et al. 2011). The distance between landmarks 3 and 13 was used to estimate wing length (Debat et al. 2011) (Supplementary Figure 1). Each measurement was taken twice. Genetic interactions between individual genes and *CycG*$^{\Delta P}$ were tested using the same protocol.

FA of wing length was estimated using the FA10 index as previously described (Debat et al. 2011). The nortest package was used to test normality of the difference between left- and right-wing size (Shapiro-Wilk and Lilliefors tests) as well as skewness and kurtosis. The rare outliers that perturbated normality, skewness (< -0.5 or > +0.5) or kurtosis (< -3 or > +3) were eliminated from the sample (see number of individuals in Supplementary

Table 3). F-tests were performed to compare FA of the assays to the one of the series internal controls (*Df/da-Gal4*, *UAS-CycG*$^{\Delta P}$ compared to *+/da-Gal4*, *UAS-CycG*$^{\Delta P}$, *Df/da-Gal4* compared to *+/da-Gal4*). Holm-Bonferroni correction was applied to each series. Inter-individual variance of wing length represented the variance of the individual mean wing length in the same population.

RESULTS

Genome-wide screen for deficiencies that modify *CycG*-induced fluctuating asymmetry

To scan the whole genome for modification of *CycG*$^{\Delta P}$-induced FA, we used a set of 499 deficiencies uncovering approximately 90% of the euchromatic genome (Supplementary Table 1). Of these, 4 deficiencies were too weak to be crossed (Supplementary Table 1). A primary screen was performed by crossing females of the remaining 495 deficiencies with *da-Gal4*, *UAS-CycG*$^{\Delta P}$*/TM6c, Sb* males (Supplementary Figure 1). As the FA values varied from experiment to experiment, a positive control (*w* females crossed with *da-Gal4*, *UAS-CycG*$^{\Delta P}$*/TM6c,Sb* males) and a negative control (*w* females crossed with *da-Gal4/TM6c,Sb* males) were systematically included in each experimental series to serve as intrinsic standards. Forty-one deficiencies were lethal or sub-lethal when combined with the *da-Gal4*, *UAS-CycG*$^{\Delta P}$ chromosome, preventing FA analyses (Supplementary Table 1). Two deficiencies produced damaged wings when combined with *da-Gal4*, *UAS-CycG*$^{\Delta P}$, rendered them unmeasurable (Supplementary Table 1). A total of 16,200 fly wings were mounted and analysed in this primary screen. Of the 452 deficiencies whose combination with *da-Gal4*, *UAS-CycG*$^{\Delta P}$ produced viable flies with usable wings, most did not modify *CycG*$^{\Delta P}$-induced FA (neutral deficiencies). However, 39 deficiencies and 21 significantly decreased or increased *CycG*$^{\Delta P}$-induced FA, respectively (Supplementary Table 1). We then performed a secondary screen by crossing females of these 60 deficiencies with *da-Gal4*, *UAS-CycG*$^{\Delta P}$*/TM6c,Sb* or *da-Gal4* males in order to replicate the primary screen while measuring the FA of the deficiencies independently of *CycG*$^{\Delta P}$ overexpression. In addition, 8 neutral deficiencies were randomly selected to confirm the absence of an effect. The results of this secondary screen – a total of 4640 fly wings were mounted and analysed – are shown in Supplementary Table 3. Of the 68 deficiencies tested, only three, *Df(2L)BSC17*, *Df(1)BSC582*, and *Df(3L)BSC419*, increased FA when combined with *da-Gal4* in absence of *CycG*$^{\Delta P}$ expression. None decreased it. Nevertheless, the increase was

rather modest compared to that observed in context of *CycG*$^{\Delta P}$ expression (3.3, 3.4 and 4.8 *versus* 28.5, 73.4 and 73.4 for the intrinsic positive controls, respectively). Interestingly, *Df(3L)BSC419* partially overlaps *Df(3L)ED4978*, which has already been shown to increase wing shape and bristle FA (Takahashi, Okada, Teramura, et al. 2011; Takahashi, Okada, and Teramura 2011). The absence of *CycG*$^{\Delta P}$-induced FA modification was verified for the 8 neutral deficiencies. However, the secondary screen eliminated some deficiencies whose effect on *CycG*$^{\Delta P}$-induced FA was no longer significant, probably due to the variability of the internal control. Thus, the screen ended with 29 modifier deficiencies: 16 that reproducibly decreased *CycG*$^{\Delta P}$-induced FA and 13 that reproducibly enhanced it, further referred to as decreasing (D) and enhancing (E) deficiencies, respectively (Table 1 and Figure 1). We did not observe any significant correlation between the size of these deficiencies and the amplitude of their effect on *CycG*$^{\Delta P}$-induced FA (Figure 2A).

Surprisingly, the 13 E deficiencies clustered on the second chromosome and the left arm of the third chromosome whereas the 16 D deficiencies clustered on the X chromosome and the right arm of the third chromosome (Table 1). The mean wing size of all *Df; da-Gal4*, *UAS-CycG*$^{\Delta P}$ flies was smaller than that of *Df; da-Gal4* flies, indicating that *CycG*$^{\Delta P}$ expression had a dominant effect on size reduction (Figure 2B and Supplementary Figure 2). Lastly, we observed a positive correlation between FA and inter-individual variance (Figure 2C). As environmental conditions cannot be fully controlled and individuals are not genetically perfectly identical, this inter-individual variance thus reflects minute genetic and environmental differences. Whether organisms are simultaneously robust to developmental noise, environmental and genetic effects is unclear. This positive correlation between FA and inter-individual variance suggests a match between developmental stability and environmental/genetic robustness.

Taken together, these results confirmed that *CycG*$^{\Delta P}$ expression strongly perturbs developmental stability. In addition, we identified 29 deficiencies among the 452 analysed that enhanced or decreased *CycG*$^{\Delta P}$-induced FA and could thus contain genes important for developmental stability. These genes could therefore be partners of *CycG* in the mechanisms that maintain developmental stability.

Identification of genes that modify *CycG*$^{\Delta P}$-induced fluctuating asymmetry

We next set out to identify partners of *CycG* in developmental stability within these deficiencies. Interestingly, *Df(3R)ED6361*, which uncovers *CycG*, reduced the FA induced

by *CycG*$^{\Delta P}$ expression, suggesting that expression of *CycG*$^{\Delta P}$ behaved as a dominant negative mutant and that the deviation from symmetry it induced was dose-dependent. Taken together, the E deficiencies contained 736 genes (576 protein-coding genes and 160 non-protein-coding genes), and the D deficiencies 865 genes (715 protein-coding genes and 150 non-protein-coding genes), making it impossible to test mutants of these genes individually. To select which mutants to test, we focused on genes encoding direct protein partners of Cyclin G or genes involved in the control of growth (Supplementary Table 2).

Although located in D deficiencies (Supplementary Table 3), mutants or RNAi lines for *Aladin* (Carvalhal et al. 2015), *CG9426* (FBgn0032485)*, E5* (Dalton et al. 1989), *eEF2* (Marygold et al. 2017), and *SAK* (Bettencourt-Dias et al. 2004) which encode direct Cyclin G physical interactors, significantly increased *CycG*$^{\Delta P}$-induced FA (Figure 3). Other genes, or combinations of genes, in these deficiencies may be responsible for the observed effects. On the other hand, two RNAi lines for *larp*, which is located in a D deficiency (*Df(3R)BSC322*) and also encodes a direct Cyclin G physical interactor (11), significantly reduced *CycG*$^{\Delta P}$-induced FA (Figure 3). Larp and Cyclin G may thus be direct partners in a process important for developmental stability.

The Hippo signalling pathway plays a key role in controlling organ size (10). *Merlin* (*Mer*), which encodes a positive regulator of this pathway that interacts directly with Cyclin G (11), is located in the D deficiency *Df(1)BSC871*. Additionally, *hippo* (*hpo*), which encodes the kinase of the pathway, is located in *Df(2R)ED3728*, which increased *CycG*$^{\Delta P}$-induced FA. This prompted us to investigate the impact of other members of the Hippo pathway on *CycG*$^{\Delta P}$-induced FA. Mutants for *Mer, hpo, ft*, *exp*, *wts* and *ban*, significantly increased it (Figure 4A). Furthermore, *Mer* inactivation also increased FA independently of *CycG* deregulation (Figure 4A). These results suggest that the Hippo pathway plays a role in developmental stability.

The *mTor* gene, which encodes the central member of another key regulator of growth (Grewal 2009), the InsulinR/TOR signalling pathway (InR/TOR) belongs to a deficiency that reduced *CycG*$^{\Delta P}$-induced FA [*Df(2L)BSC277*]. Furthermore, Cyclin G interacts directly with three actors of this pathway : Akt1, PP2A and Wdb (Fischer et al. 2016; Oughtred et al. 2021). We thus tested the effect of *mTor* and other members of the pathway for their effect on *CycG*$^{\Delta P}$-induced FA. Most of these, particularly mutants for *Akt1*, *S6K*, *foxo*, *PTEN*, *mTor* and *wdb*, increased *CycG*$^{\Delta P}$-induced FA. This suggests that the interaction between Cyclin G and the InR/TOR pathway is crucial for developmental stability

(Figure 4B).

Finally, two major morphogens of the wing, *dpp* and *wg* [for a review see (Tabata and Takei 2004)], belonged to deficiencies that enhanced *CycG*$^{\Delta P}$-induced FA [*Df(2L)Exel7011* and *Df(2L)BSC291*, respectively]. Mutants for both genes also increased *CycG*$^{\Delta P}$-induced FA, indicating that we had identified at least one gene responsible for this effect within each deficiency (Figure 4C).

DISCUSSION

In our efforts to identify deficiencies that modify *CycG*$^{\Delta P}$-induced FA, we found that 13 deficiencies out of 452 enhanced it (E deficiencies) while 16 deficiencies decreased it (D deficiencies). Notably, these deficiencies were not evenly distributed across all chromosomes. The D deficiencies were enriched on chromosomes X and 3R, whereas the E deficiencies were concentrated on chromosomes 2 and 3L. This pattern suggests that chromosomes 2 and 3L may have a general positive effect on developmental stability. In addition, we observed that the vast majority of modifier deficiencies (65 out of the 68 tested) does not affect FA on their own. Finally, the 13 deficiencies that enhance *CycG*$^{\Delta P}$-induced FA represent only 4.1 % of the *Drosophila melanogaster* genome. Collectively, these results indicate that under normal rearing conditions the control of growth is highly robust.

Overexpression of *CycG*$^{\Delta P}$ using the Gal4/UAS system provides an entry point to discover genes and gene networks that are essential for growth homeostasis. Not surprisingly, we found that the major morphogens (Dpp and Wg) and growth pathways (InR/Tor and Hippo pathways) are essential for developmental stability. In line with our findings, alternative splicing of *yki*, which encodes the transcription factor Yorkie, a target of the Hippo pathway, has previously been shown to contribute to developmental stability (Srivastava et al. 2020 Dec 15). Furthermore, Merlin that promotes assembly of a functional Hippo signaling complex at the apical cell cortex has been shown to directly interact with Cyclin G (Oughtred et al. 2021). Beyond its specific role, Cyclin G may be unique in that it sits at the crossroads of many signalling pathways. Our previous systems biology approach has indeed shown that *CycG* is linked to many genes in the wing imaginal disc (Dardalhon-Cuménal et al. 2018). These new findings confirm that *CycG* may be a hub within a complex genetic network important for the robustness of organ growth. We have previously

shown that expression of *CycG*$^{\Delta P}$ abolishes the strong negative correlation between cell size and cell number observed in wild-type fly wings (Debat et al. 2011). Cyclin G may orchestrate growth homeostasis by ensuring the proper coordination of growth and the cell cycle, which would be critical for developmental stability. This central role may explain the spectacular effects of its deregulation on fluctuating asymmetry.

Some potential direct Cyclin G partners are included in the deficiencies that modify *CycG*$^{\Delta P}$-induced FA. Strikingly, these partners belong to different gene ontology categories, ranging from the aforementioned Merlin to transcription factors (*e.g.* E5), translation regulators (*e.g.* Larp) and proteins involved in protein degradation (*e.g.* Cul2), reinforcing the idea that Cyclin G may be involved in diverse cellular processes. Among the genes encoding these potential direct partners, *larp* is the only one whose inactivation strongly reduces *CycG*$^{\Delta P}$-induced FA, suggesting that the effect of Cyclin G on FA requires this direct interaction. *Larp* encodes an evolutionarily conserved RNA-binding protein that forms a complex with the Poly(A) binding protein (PABP), a translation regulator (Blagden et al. 2009; Deragon and Bousquet- Antonelli 2015). In addition, Larp recognises mRNAs with a 5' Terminal OligoPyrimidine (5' TOP) motif, *i.e.* mRNAs encoding proteins essential for protein synthesis such as ribosomal proteins or translation factors (Cockman et al. 2020). More recently, Larp has been shown to play a dual role as a translational repressor and a stabiliser of 5' TOP mRNAs (20). In particular, when phosphorylated by Pink1, Larp inhibits translation at the mitochondrial outer membrane suggesting that it may have an effect on the production of new mitochondria(Zhang et al. 2019). Interestingly, in wing imaginal discs expressing *CycG*$^{\Delta P}$, genes involved in translation are up-regulated and those involved in metabolism and mitochondrial activity are down-regulated (Dardalhon-Cuménal et al. 2018). Taken together, these data support the idea that there may be a link between developmental stability and the regulation of mitochondrial activity.

FIGURES

Figure 1: Secondary screen – Analysis of the 60 candidate deficiencies isolated from the primary screen.

a – FA of 39 deficiencies that decreased *CycG*$^{\Delta P}$-induced FA in the primary screen

normalised to the FA of *da-Gal4, UAS-CycG$^{\Delta P}$* (red line). 16 of them reproduced the results of the primary screen (orange).

b – FA of 21 deficiencies that enhanced *CycG$^{\Delta P}$*-induced FA in the primary screen normalised to the FA of *da-Gal4, UAS-CycG$^{\Delta P}$* (red line). 13 of them reproduced the results of the primary screen (green).

*p<0.05, **p<0.01, ***p<0.001

Figure 2: Secondary screen - Relationship between fluctuating asymmetry and deficiency length, mean wing size and inter-individual variance.

a – FA (fold change) of the 16 decreasing (D) deficiencies (orange), the 13 enhancing (E) deficiencies (green) and 8 neutral deficiencies (grey) versus deficiency length. No significant correlation was observed between the two parameters (Pearson coefficient, R= -0.15).

b - FA of the 16 decreasing (D) deficiencies (orange) and the 13 enhancing (E) deficiencies (green) combined with *da-Gal4, UAS-CycG$^{\Delta P}$* (filled circles) or not (empty circles) versus mean wing size. Filled grey square: *+/da-Gal4, UAS-CycG$^{\Delta P}$*; empty grey square: *+/da-Gal4*. A strong negative correlation was observed between these parameters (R= -0.65).

c – FA (log10) of the 16 decreasing (D) deficiencies (orange) and the 13 enhancing (E) deficiencies (green) combined with *da-Gal4, UAS-CycG$^{\Delta P}$* (filled circles) or not (empty circles) versus inter-individual variance (log10). Filled grey square: *+/da-Gal4, UAS-CycG$^{\Delta P}$*; empty grey square: *+/da-Gal4*. A strong positive correlation was observed between the two parameters (R= +0.67).

Figure 3: Candidate gene analyses – Genes encoding direct protein partners of Cyclin G located in deficiencies that modify *CycG$^{\Delta P}$*-induced FA.

In green, alleles that significantly increased *CycG$^{\Delta P}$*-induced FA**.** In orange, alleles that significantly decreased *CycG$^{\Delta P}$*-induced FA. In light grey, positive control *(+/da-Gal4, UAS-CycG$^{\Delta P}$*). In dark grey, alleles that did not modify *CycG$^{\Delta P}$*-induced FA. Several alleles were lethal (†) when combined to *+/da-Gal4* or *+/da-Gal4, UAS-CycG$^{\Delta P}$*.

*p<0.05, **p<0.01, ***p<0.001

Figure 4: Candidate gene analyses – Genes encoding members of the Hippo pathway

(a), the InR/TOR pathway (b) and the Dpp and Wg morphogens (c).
In green, alleles that significantly increased *CycG*$^{\Delta P}$-induced FA**.** In grey, alleles that did not modify *CycG*$^{\Delta P}$-induced FA.
*p<0.05, **p<0.01, ***p<0.001

Supplementary Figure 1:
a - Position of the 15 landmarks on the wing. Landmarks 3 and 13 (red) were used to measure wing length.
b – Diagrams of primary and secondary screens.
Df: deficiency; *w*^{n}: *w*^{5905} or *w*^{6326}; *Bal*: balancer chromosome; N: neutral deficiencies; D: deficiency that decreased *CycG*$^{\Delta P}$-induced fluctuating asymmetry; E: deficiency that increased *CycG*$^{\Delta P}$-induced fluctuating asymmetry.

Supplementary Figure 2: Secondary screen – Mean wing size of flies heterozygous for the deficiencies associated with *da-Gal4* (top) or *da-Gal4, UAS-CycG*$^{\Delta P}$ (down).
Box-plots showing mean wing size. In grey, mean wing size of *+/da-Gal4* (**a**) or *+/da-Gal4, UAS-CycG*$^{\Delta P}$ flies. In orange, mean wing size of deficiencies that decreased *CycG*$^{\Delta P}$-induced FA combined with *da-Gal4* (top) or *da-Gal4, UAS-CycG*$^{\Delta P}$ (down). In green, mean wing size of deficiencies that increased *CycG*$^{\Delta P}$-induced FA combined with *da-Gal4* (top) *or da-Gal4, UAS-CycG*$^{\Delta P}$ (**b**).
The two red lines correspond to the mean wing size of *+/da-Gal4* (1161) and *+/da-Gal4, UAS-CycG*$^{\Delta P}$ (1014) flies.
*p<0.05, **p<0.01, ***p<0.001

Table 1: Deficiencies modifying *CycG$^{\Delta P}$*-induced FA.

The fluctuating asymmetry fold-change corresponds to the ratio between fluctuating asymmetry of the deficiency combined to *da-Gal4, UAS-CycG$^{\Delta P}$* and fluctuating asymmetry of *da-Gal4, UAS-CycG$^{\Delta P}$*.

Chromosome arm	Deficiency name	Cytological location	Fluctuating asymmetry fold-change	Adjusted p-value
X	*Df(1)BSC530*	1A5;1B12	0.37329	4.68E-02
	Df(1)M38-C5	8B;8E	0.24024	2.86E-03
	Df(1)BSC722	10B3;10E1	0.25570	6.72E-03
	Df(1)FDD-0024486	14C4;14D1	0.12722	2.58E-06
	Df(1)BSC643	15F9;16F1	0.28609	7.33E-03
	Df(1)BSC405	16D5;16F6	0.37682	4.68E-02
	Df(1)BSC871	18D7;18F2	0.32513	2.55E-02
2L	*Df(2L)Exel7011*	22E1;22F3	3.67005	4.34E-03
	Df(2L)BSC354	26D7;26E3	4.32949	1.32E-03
	Df(2L)BSC291	27D6;27F2	2.69177	3.96E-02
	Df(2L)Exel7034	28E1;28F1	3.92670	2.69E-03
	Df(2L)ED629	29B4;29E4	6.02764	5.81E-05
	Df(2L)BSC277	34A1;34B2	0.39515	2.82E-02
	Df(2L)ED1473	39B4;40A5	3.37401	7.77E-03
	Df(2L)lt109	h35;h35	2.87894	2.34E-02
2R	*Df(2R)BSC880*	49A9;49E1	3.36810	9.85E-04
	Df(2R)ED3728	56D10;56E2	2.79286	2.50E-02
3L	*Df(3L)ED201*	61B1;61C1	9.14411	6.11E-07
	Df(3L)ED4457	67E2;68A7	3.77715	3.03E-03
	Df(3L)BSC12	69F6;70A2	7.46921	5.43E-06
	Df(3L)ED4710	74D1;75B11	5.14760	1.95E-04
	Df(3L)BSC419	78C2;78D8	0.20077	5.30E-04
3R	*Df(3R)BSC549*	83A6;83B6	0.28288	9.98E-03
	Df(3R)ED5623	87E3;88A4	0.32086	1.65E-02
	Df(3R)ED5705	88E12;89A5	0.33282	1.69E-02
	Df(3R)ED6255	97D2;97F1	0.27386	5.53E-03
	Df(3R)BSC322	98C3;98D7	0.33719	3.21E-02
	Df(3R)BSC749	100B1;100C1	0.39540	9.04E-03
	Df3R)ED6361	100C7;100E3	0.40559	1.17E-02

Supplementary Table 1: Deficiencies used in this study.

Supplementary Table 2: Alleles used in this study to identify genes that modify *CycG*$^{\Delta P}$-induced fluctuating asymmetry.

Supplementary Table 3: Secondary screen for deficiencies which modify *CycG*$^{\Delta P}$-induced FA.

Data availability statement

The authors confirm that all the data necessary to verify the conclusions of the article are included in the text, figures and tables. Strains are available upon request.

Acknowledgments

The authors would like to thank all the members of the Heterochromatin, Cell Fate and Exposome team for their valuable advice and productive discussions. They would also like to thank Dr. Y. Bellaïche for providing the *Akt1[1]* mutant, and the Bloomington Stock Center for mutant and deficiency strains.

Study funding

This study was funded by ongoing support from the Centre National de la Recherche Scientifique (CNRS) and Sorbonne Université (SU).

REFERENCES

Debat V. 2001. Mapping phenotypes: canalization, plasticity and developmental stability. Trends in Ecology & Evolution. 2001;16:555–561.

Leamy L et al. 2015. The Genetic Architecture of Fluctuating Asymmetry of Mandible Size and Shape in a Population of Mice: Another Look. Symmetry. 2015;7(1):146–163. https://doi.org/10.3390/sym7010146

Takahashi KH, Okada Y, Teramura K, Tsujino M. 2011. Deficiency mapping of the genomic regions associated with effects on developmental stability in Drosophila melanogaster. Evolution. 2011;65:3565–3577.

Takahashi KH, Okada Y, Teramura K. 2011. Genome-Wide Deficiency Mapping of the Regions Responsible for Temporal Canalization of the Developmental Processes of Drosophila melanogaster. J Hered. 2011;102(4):448–57. https://doi.org/10.1093/jhered/esr026

Debat V et al. 2011. Developmental Stability: A Major Role for Cyclin G in Drosophila melanogaster. PLoS Genet. 2011;7(10):e1002314. https://doi.org/10.1371/journal.pgen.1002314

Debat V, Peronnet F. 2013. Asymmetric flies: The control of developmental noise in Drosophila. Fly (Austin). 2013;7(2):1–8. https://doi.org/10.4161/fly.23558

Carvalhal S et al. 2015. The nucleoporin ALADIN regulates Aurora A localization to ensure robust mitotic spindle formation Zheng Y, editor. Molecular Biology of the Cell. 2015 [accessed 2025 Jun 5];26(19):3424–3438. https://www.molbiolcell.org/doi/10.1091/mbc.E15-02-0113. https://doi.org/10.1091/mbc.E15-02-0113

Dalton D, Chadwick R, McGinnis W. 1989. Expression and embryonic function of empty spiracles: a Drosophila homeo box gene with two patterning functions on the anterior-posterior axis of the embryo. Genes & Development. 1989 [accessed 2024 Nov 11];3(12a):1940–1956. http://www.genesdev.org/cgi/doi/10.1101/gad.3.12a.1940. https://doi.org/10.1101/gad.3.12a.1940

Marygold SJ, Attrill H, Lasko P. 2017. The translation factors of Drosophila melanogaster. Fly (Austin). 2017;11(1):65–74. https://doi.org/10.1080/19336934.2016.1220464

Bettencourt-Dias M et al. 2004. Genome-wide survey of protein kinases required for cell cycle progression. Nature. 2004;432(7020):980–7. https://doi.org/10.1038/nature03160

Grewal SS. 2009. Insulin/TOR signaling in growth and homeostasis: a view from the fly world. Int J Biochem Cell Biol. 2009;41(5):1006–10. https://doi.org/10.1016/j.biocel.2008.10.010

Fischer P, Preiss A, Nagel AC. 2016. A triangular connection between Cyclin G, PP2A and Akt1 in the regulation of growth and metabolism inDrosophila. Fly. 2016:1–8. https://doi.org/10.1080/19336934.2016.1162362

Oughtred R et al. 2021. The BIOGRID database: A comprehensive biomedical resource of curated protein, genetic, and chemical interactions. Protein Science. 2021 [accessed 2024 Nov 2];30(1):187–200. https://onlinelibrary.wiley.com/doi/10.1002/pro.3978. https://doi.org/10.1002/pro.3978

Tabata T, Takei Y. 2004. Morphogens, their identification and regulation. Development. 2004 [accessed 2024 Nov 11];131(4):703–712. https://journals.biologists.com/dev/article/131/4/703/42586/Morphogens-their-identification-and-regulation. https://doi.org/10.1242/dev.01043

Srivastava D et al. 2020. Modulation of Yorkie activity by alternative splicing is required for developmental stability. The EMBO Journal. 2020 Dec 15 [accessed 2020 Dec 28]. https://onlinelibrary.wiley.com/doi/10.15252/embj.2020104895. https://doi.org/10.15252/embj.2020104895

Dardalhon-Cuménal D et al. 2018. Cyclin G and the Polycomb Repressive complexes PRC1 and PR-DUB cooperate for developmental stability. PLoS Genet. 2018;14(7):e1007498. https://doi.org/10.1371/journal.pgen.1007498

Blagden SP et al. 2009. Drosophila Larp associates with poly(A)-binding protein and is required for male fertility and syncytial embryo development. Developmental Biology. 2009 [accessed 2025 Feb 9];334(1):186–197. https://linkinghub.elsevier.com/retrieve/pii/S0012160609010665. https://doi.org/10.1016/j.ydbio.2009.07.016

Deragon J, Bousquet-Antonelli C. 2015. The role of LARP1 in translation and beyond. WIREs RNA. 2015 [accessed 2024 Nov 11];6(4):399–417. https://wires.onlinelibrary.wiley.com/doi/10.1002/wrna.1282. https://doi.org/10.1002/wrna.1282

Cockman E, Anderson P, Ivanov P. 2020. TOP mRNPs: Molecular Mechanisms and Principles of Regulation. Biomolecules. 2020 [accessed 2025 Feb 9];10(7):969. https://www.mdpi.com/2218-273X/10/7/969. https://doi.org/10.3390/biom10070969

Berman AJ et al. 2021. Controversies around the function of LARP1. RNA Biology. 2021 [accessed 2024 Nov 11];18(2):207–217. https://www.tandfonline.com/doi/full/10.1080/15476286.2020.1733787. https://doi.org/10.1080/15476286.2020.1733787

Zhang Y et al. 2019. PINK1 Inhibits Local Protein Synthesis to Limit Transmission of Deleterious Mitochondrial DNA Mutations. Molecular Cell. 2019 [accessed 2022 Jun 6];73(6):1127-1137.e5. https://linkinghub.elsevier.com/retrieve/pii/S1097276519300139. https://doi.org/10.1016/j.molcel.2019.01.013

Figure 1

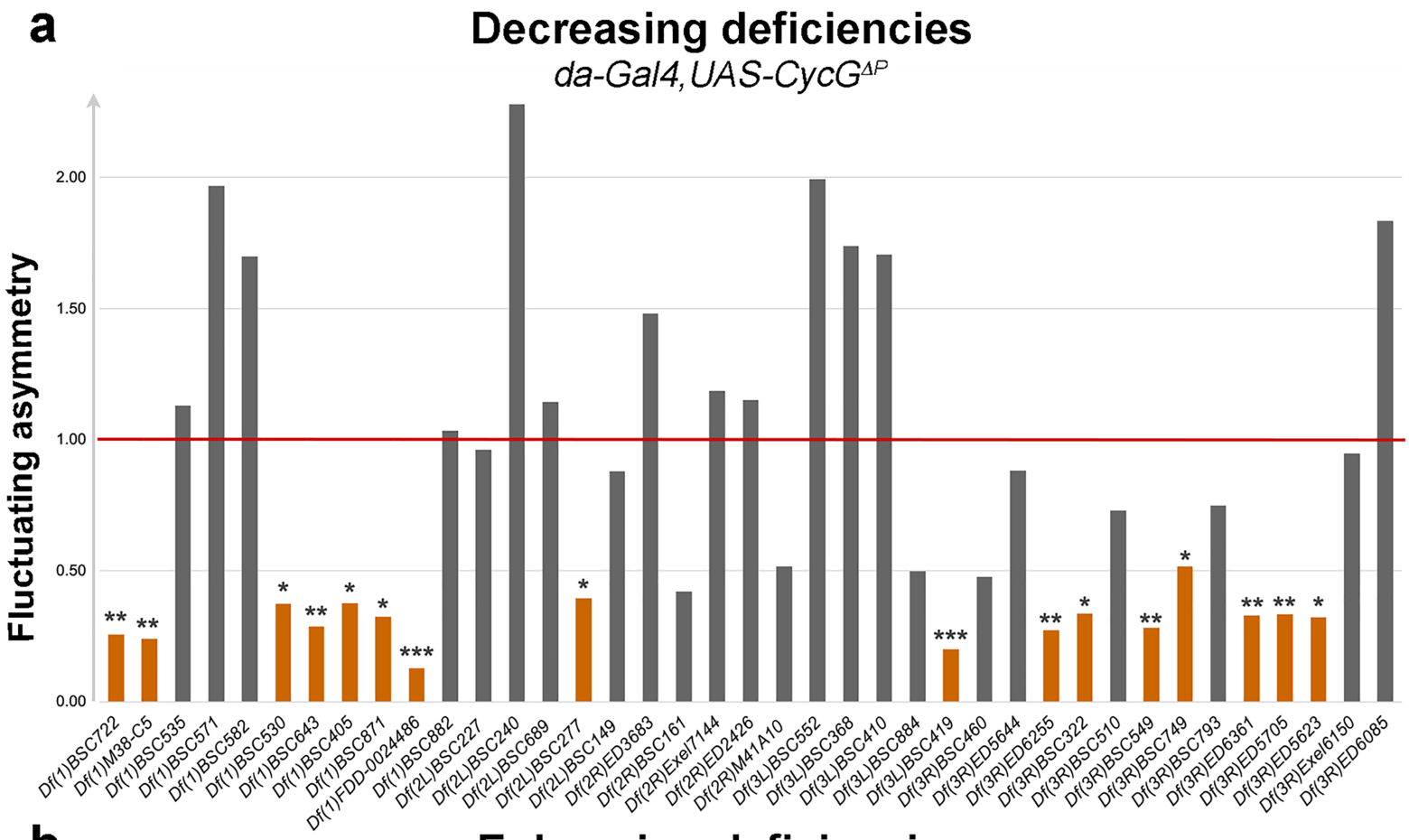
a
Decreasing deficiencies
da-Gal4,UAS-CycG^ΔP
Fluctuating asymmetry
0.00
0.50
1.00
1.50
2.00
Df(1)BSC722
Df(1)M38-C5
Df(1)BSC535
Df(1)BSC571
Df(1)BSC582
Df(1)BSC530
Df(1)BSC643
Df(1)BSC405
Df(1)BSC871
Df(1)FDD-0024486
Df(1)BSC882
Df(2L)BSC227
Df(2L)BSC240
Df(2L)BSC689
Df(2L)BSC277
Df(2L)BSC149
Df(2R)ED3683
Df(2R)BSC161
Df(2R)Exel7144
Df(2R)ED2426
Df(2R)M41A10
Df(3L)BSC552
Df(3L)BSC368
Df(3L)BSC410
Df(3L)BSC884
Df(3L)BSC419
Df(3R)BSC460
Df(3R)ED5644
Df(3R)ED6255
Df(3R)BSC322
Df(3R)BSC510
Df(3R)BSC549
Df(3R)BSC749
Df(3R)BSC793
Df(3R)ED6361
Df(3R)ED5705
Df(3R)ED5623
Df(3R)Exel6150
Df(3R)ED6085

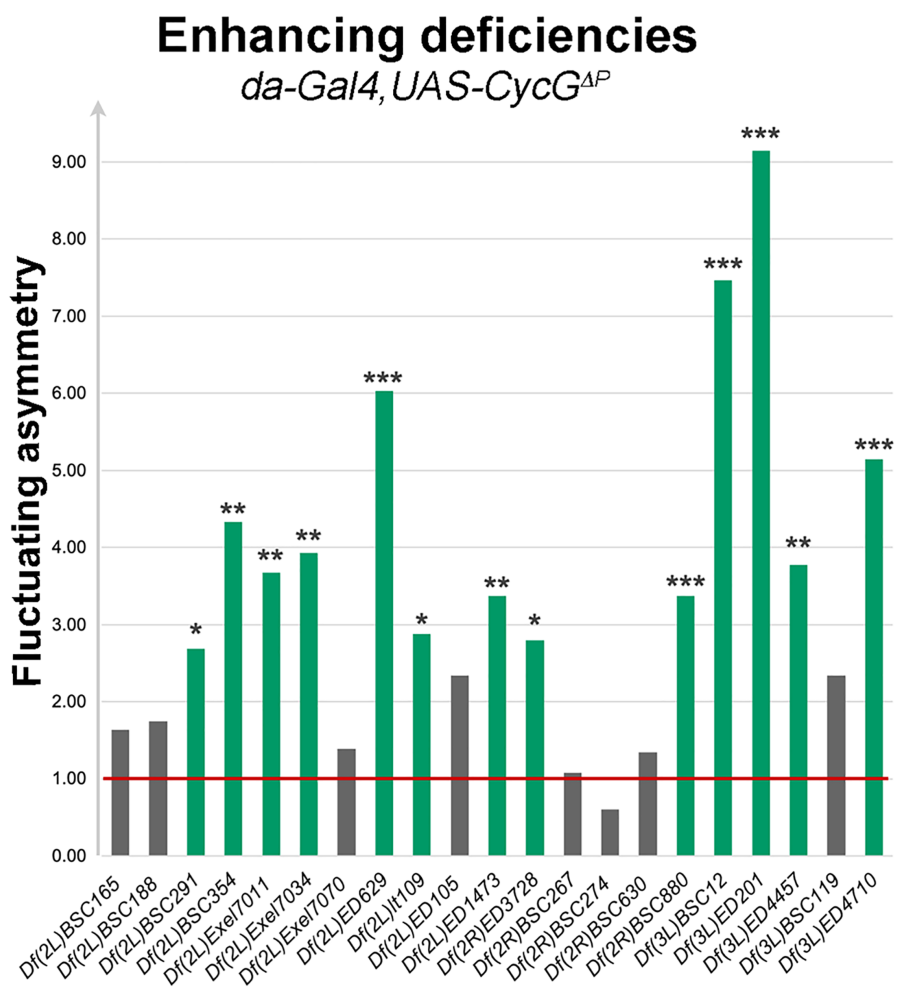
b
Enhancing deficiencies
da-Gal4,UAS-CycG^ΔP
Fluctuating asymmetry
0.00
1.00
2.00
3.00
4.00
5.00
6.00
7.00
8.00
9.00
Df(2L)BSC165
Df(2L)BSC188
Df(2L)BSC291
Df(2L)BSC354
Df(2L)Exel7011
Df(2L)Exel7034
Df(2L)Exel7070
Df(2L)ED629
Df(2L)lt109
Df(2L)ED105
Df(2L)ED1473
Df(2R)ED3728
Df(2R)BSC267
Df(2R)BSC274
Df(2R)BSC630
Df(2R)BSC880
Df(3L)BSC12
Df(3L)ED201
Df(3L)ED4457
Df(3L)BSC119
Df(3L)ED4710

Figure 2

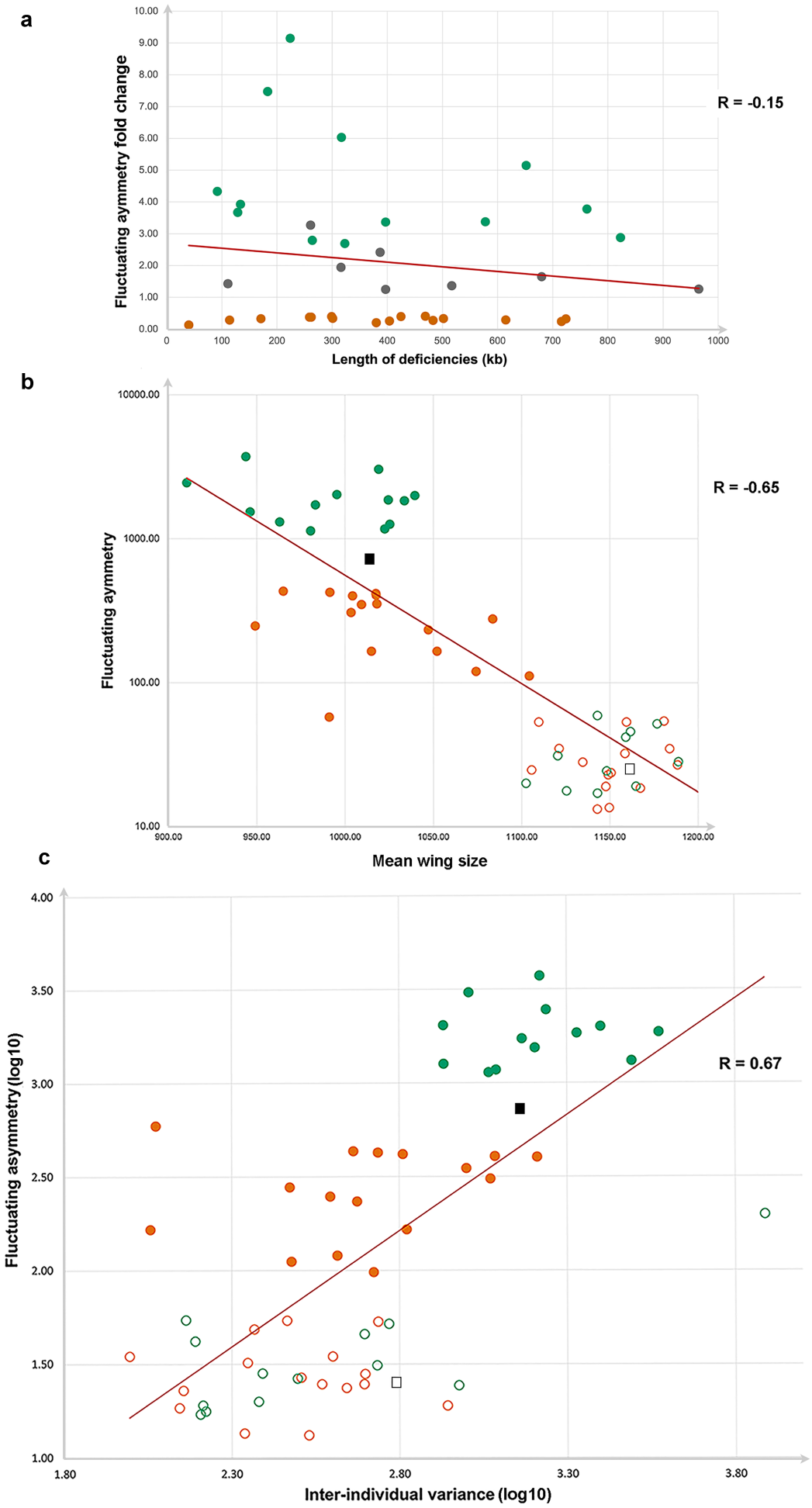
a
Fluctuating aymmetry fold change
Length of deficiencies (kb)
R = -0.15
b
Fluctuating aymmetry
Mean wing size
R = -0.65
c
Fluctuating asymmetry (log10)
Inter-individual variance (log10)
R = 0.67

Figure 3

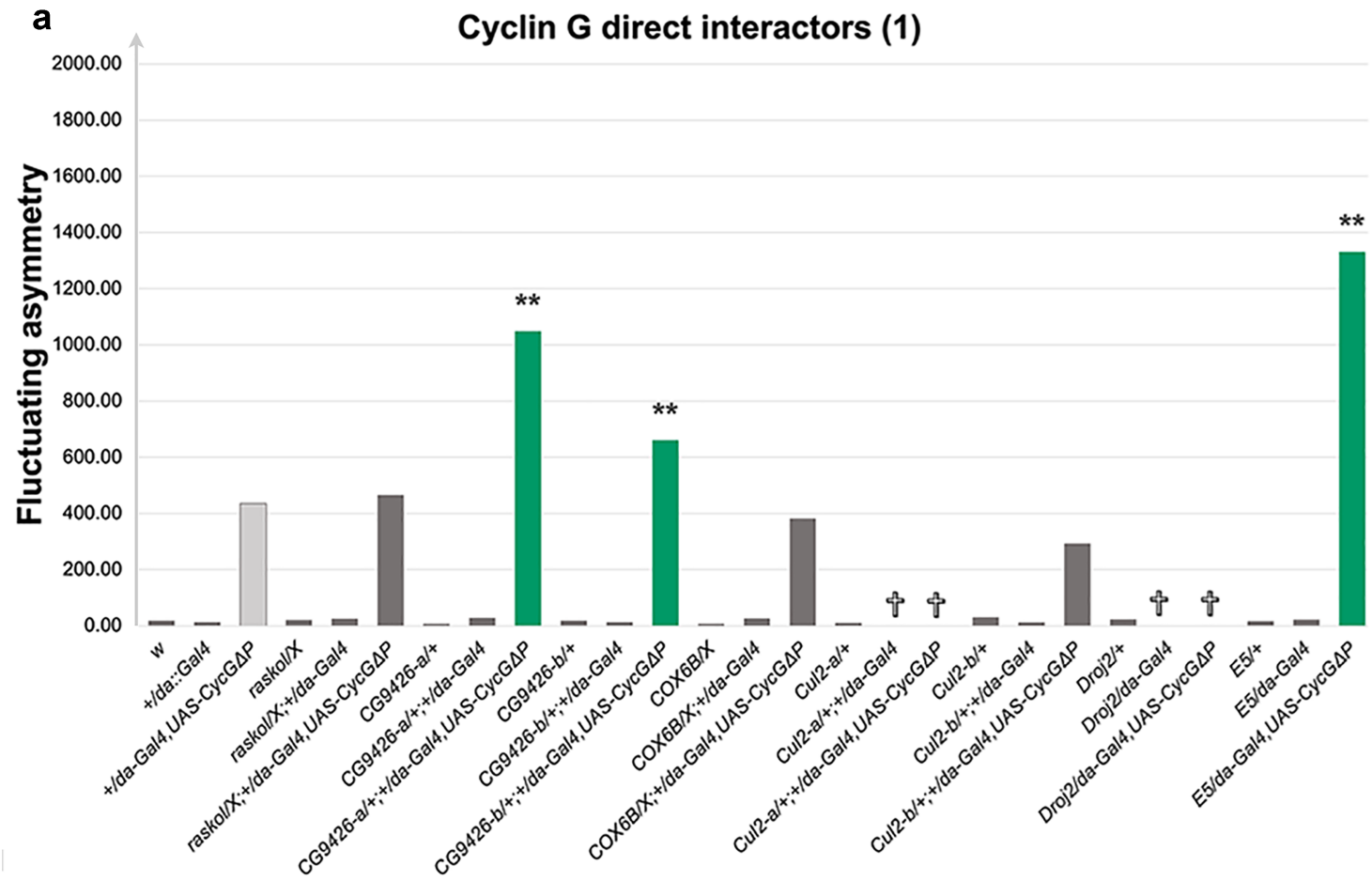
a
Cyclin G direct interactors (1)
Fluctuating asymmetry
2000.00
1800.00
1600.00
1400.00
1200.00
1000.00
800.00
600.00
400.00
200.00
0.00
**
**
**
w
+/da::Gal4
+/da-Gal4,UAS-CycGΔP
raskol/X
raskol/X;+/da-Gal4
raskol/X;+/da-Gal4,UAS-CycGΔP
CG9426-a/+
CG9426-a/+;+/da-Gal4
CG9426-a/+;+/da-Gal4,UAS-CycGΔP
CG9426-b/+
CG9426-b/+;+/da-Gal4
CG9426-b/+;+/da-Gal4,UAS-CycGΔP
COX6B/X
COX6B/X;+/da-Gal4
COX6B/X;+/da-Gal4,UAS-CycGΔP
Cul2-a/+
Cul2-a/+;+/da-Gal4
Cul2-a/+;+/da-Gal4,UAS-CycGΔP
Cul2-b/+
Cul2-b/+;+/da-Gal4
Cul2-b/+;+/da-Gal4,UAS-CycGΔP
Droj2/+
Droj2/da-Gal4
Droj2/da-Gal4,UAS-CycGΔP
E5/+
E5/da-Gal4
E5/da-Gal4,UAS-CycGΔP

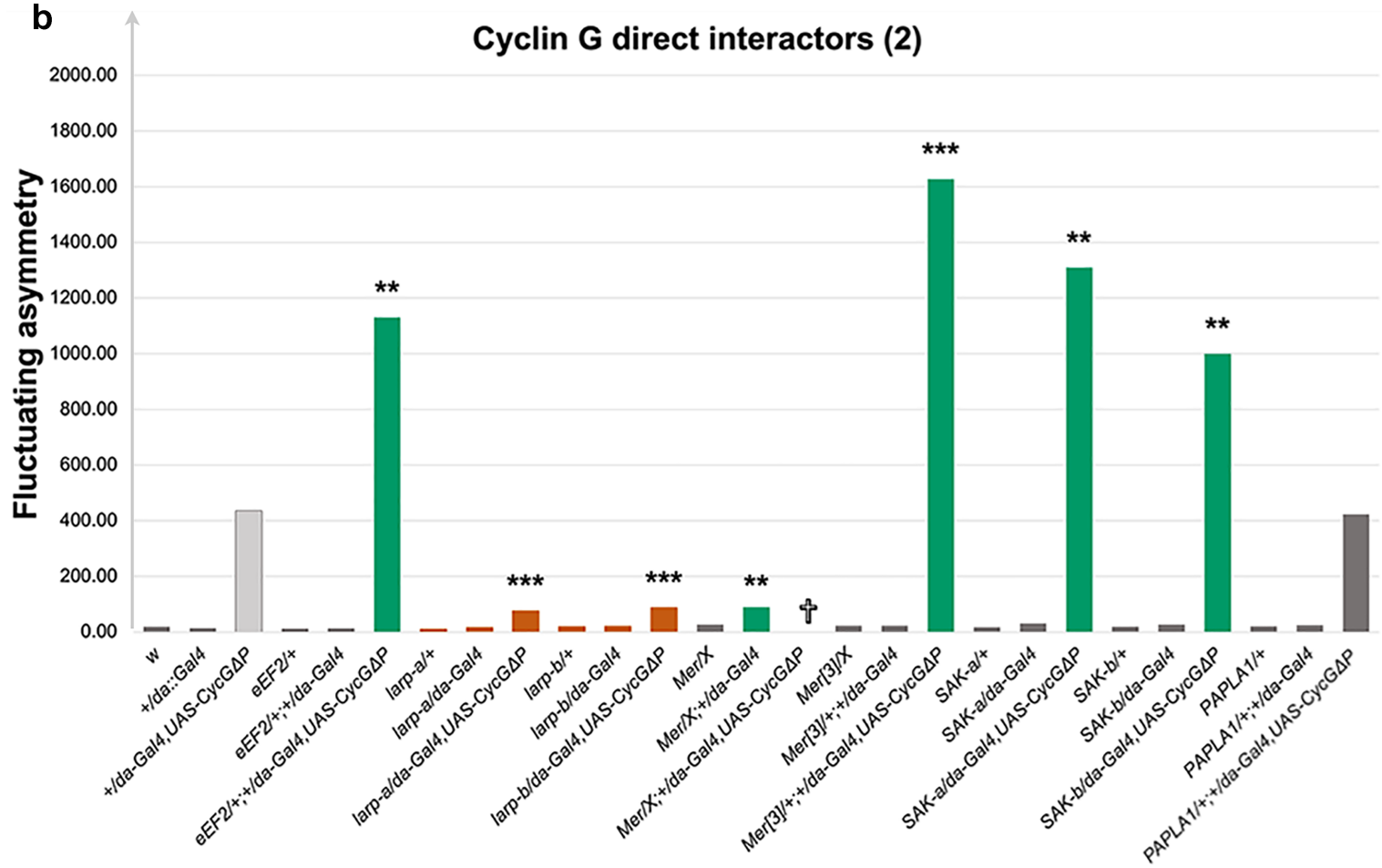
b
Cyclin G direct interactors (2)
Fluctuating asymmetry
2000.00
1800.00
1600.00
1400.00
1200.00
1000.00
800.00
600.00
400.00
200.00
0.00
**
***
***
**
***
**
**
w
+/da::Gal4
+/da-Gal4,UAS-CycGΔP
eEF2/+
eEF2/+;+/da-Gal4
eEF2/+;+/da-Gal4,UAS-CycGΔP
larp-a/+
larp-a/da-Gal4
larp-a/da-Gal4,UAS-CycGΔP
larp-b/+
larp-b/da-Gal4
larp-b/da-Gal4,UAS-CycGΔP
Mer/X
Mer/X;+/da-Gal4
Mer/X;+/da-Gal4,UAS-CycGΔP
Mer[3]/X
Mer[3]/+;+/da-Gal4
Mer[3]/+;+/da-Gal4,UAS-CycGΔP
SAK-a/+
SAK-a/da-Gal4
SAK-a/da-Gal4,UAS-CycGΔP
SAK-b/+
SAK-b/da-Gal4
SAK-b/da-Gal4,UAS-CycGΔP
PAPLA1/+
PAPLA1/+;+/da-Gal4
PAPLA1/+;+/da-Gal4,UAS-CycGΔP

Figure 4

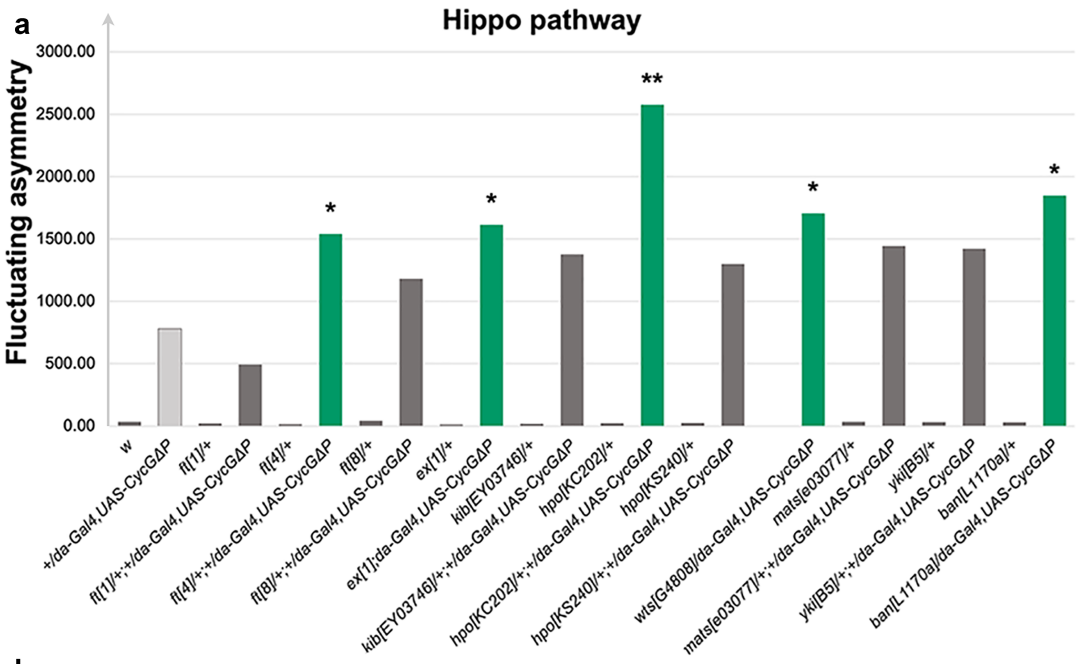
a
Hippo pathway
Fluctuating asymmetry
3000.00
2500.00
2000.00
1500.00
1000.00
500.00
0.00
w
+/da-Gal4,UAS-CycGΔP
ft[1]/+
ft[1]/+;+/da-Gal4,UAS-CycGΔP
ft[4]/+
ft[4]/+;+/da-Gal4,UAS-CycGΔP
ft[8]/+
ft[8]/+;+/da-Gal4,UAS-CycGΔP
ex[1]/+
ex[1];da-Gal4,UAS-CycGΔP
kib[EY03746]/+
kib[EY03746]/+;+/da-Gal4,UAS-CycGΔP
hpo[KC202]/+
hpo[KC202]/+;+/da-Gal4,UAS-CycGΔP
hpo[KS240]/+
hpo[KS240]/+;+/da-Gal4,UAS-CycGΔP
wts[G4808]/da-Gal4,UAS-CycGΔP
mats[e03077]/+
mats[e03077]/+;+/da-Gal4,UAS-CycGΔP
yki[B5]/+
yki[B5]/+;+/da-Gal4,UAS-CycGΔP
ban[L1170a]/+
ban[L1170a]/da-Gal4,UAS-CycGΔP

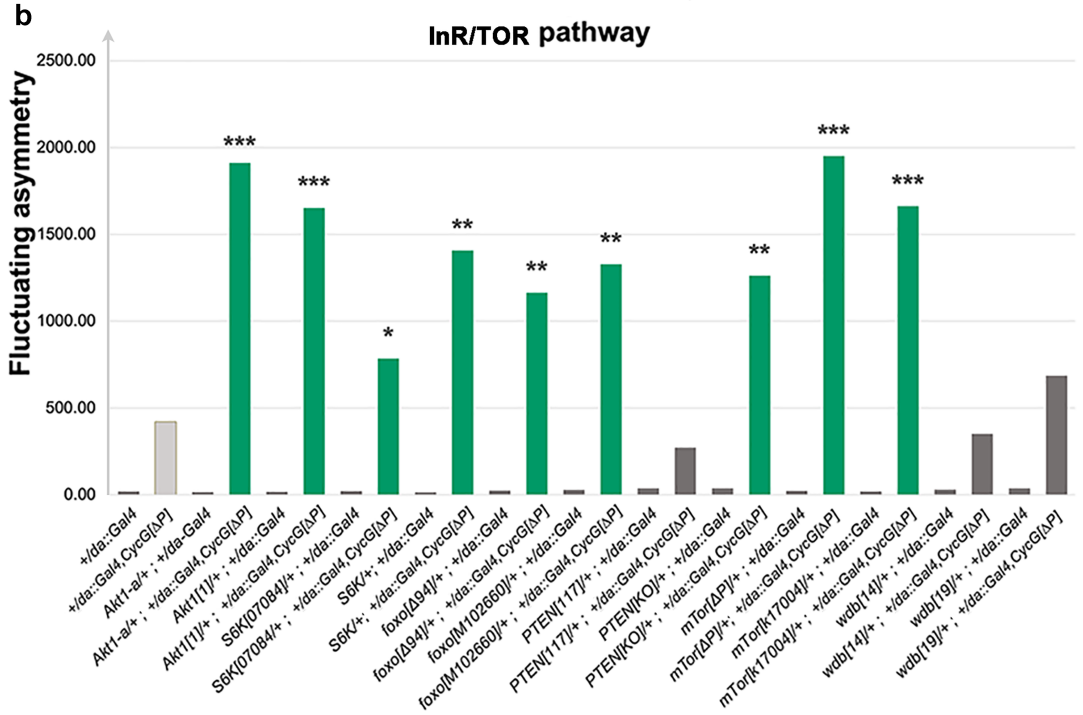
b
InR/TOR pathway
Fluctuating asymmetry
2500.00
2000.00
1500.00
1000.00
500.00
0.00
+/da::Gal4
+/da::Gal4,CycG[ΔP]
Akt1-a/+ ; +/da-Gal4
Akt1-a/+ ; +/da::Gal4,CycG[ΔP]
Akt1[1]/+ ; +/da::Gal4
Akt1[1]/+ ; +/da::Gal4,CycG[ΔP]
S6K[07084]/+ ; +/da::Gal4
S6K[07084]/+ ; +/da::Gal4,CycG[ΔP]
S6K/+; +/da::Gal4
S6K/+; +/da::Gal4,CycG[ΔP]
foxo[Δ94]/+ ; +/da::Gal4
foxo[Δ94]/+ ; +/da::Gal4,CycG[ΔP]
foxo[M102660]/+ ; +/da::Gal4
foxo[M102660]/+ ; +/da::Gal4,CycG[ΔP]
PTEN[117]/+ ; +/da::Gal4
PTEN[117]/+ ; +/da::Gal4,CycG[ΔP]
PTEN[KO]/+ ; +/da::Gal4
PTEN[KO]/+ ; +/da::Gal4,CycG[ΔP]
mTor[ΔP]/+ ; +/da::Gal4
mTor[ΔP]/+ ; +/da::Gal4,CycG[ΔP]
mTor[k17004]/+ ; +/da::Gal4
mTor[k17004]/+ ; +/da::Gal4,CycG[ΔP]
wdb[14]/+ ; +/da::Gal4
wdb[14]/+ ; +/da::Gal4,CycG[ΔP]
wdb[19]/+ ; +/da::Gal4
wdb[19]/+ ; +/da::Gal4,CycG[ΔP]

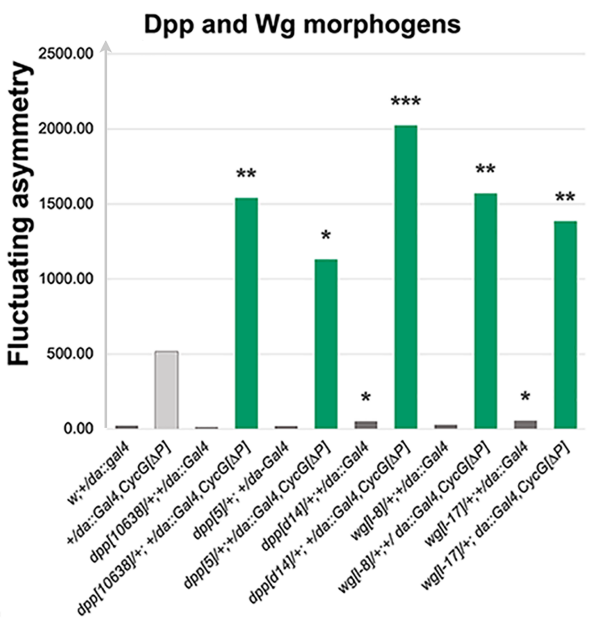
c
Dpp and Wg morphogens
Fluctuating asymmetry
2500.00
2000.00
1500.00
1000.00
500.00
0.00
w;+/da::gal4
+/da::Gal4,CycG[ΔP]
dpp[10638]/+;+/da::Gal4
dpp[10638]/+; +/da::Gal4,CycG[ΔP]
dpp[5]/+; +/da-Gal4
dpp[5]/+;+/da::Gal4,CycG[ΔP]
dpp[d14]/+;+/da::Gal4
dpp[d14]/+; +/da::Gal4,CycG[ΔP]
wg[-8]/+;+/da::Gal4
wg[-8]/+;+/ da::Gal4,CycG[ΔP]
wg[-17]/+;+/da::Gal4
wg[-17]/+; da::Gal4,CycG[ΔP]